BOND AND SPLICE BEHAVIOR OF CFRP LAMINATES FOR STRENGTHENING STEEL BEAMS

Mina Dawood[1], Sami Rizkalla[2]

[1,2]*North Carolina State University*

Abstract: This paper describes an experimental program which was conducted to investigate the bond behavior of high modulus carbon fiber reinforced polymer (CFRP) laminates. The objective of the testing was to establish an effective method to splice CFRP laminates proposed for strengthening long span steel bridges and structural members. Six double-lap shear coupons were tested to investigate various splice configurations and to investigate the suitability of different methods to reduce the bond stress concentrations which typically develop near the ends of the plates. The program also included nine steel beams that were strengthened with CFRP laminates and spliced at the midspan. Various configurations of splice cover plates were used at the midspan location to investigate the effectiveness of splicing the CFRP laminates. Several details were investigated to help reduce the bond stress concentration near the ends of the splice plate including increasing the length of the splice cover plate, implementing a reverse taper near the plate ends and applying a transverse CFRP wrap around the splice plate. All of the tested beams failed due to sudden debonding of the CFRP splice plate. The experimental results indicate that implementing the reverse tapered joint configuration can potentially reduce the shear stress concentrations near the plate ends and increase the capacity of the spliced joint. Increasing the length of the splice plate beyond a length of 400 mm did not significantly increase the splice capacity for the CFRP system that was investigated in this study. Similarly, the experimental results indicate that the presence of the transverse CFRP wrap did not increase the ultimate capacity of the spliced connection. This paper highlights the importance of proper detailing of CFRP plates to reduce bond stress concentrations and to increase the ultimate strength of bonded joints.

Keywords: *bond, splices, reverse taper, plate end debonding, high modulus CFRP*

1 Introduction

For the last ten years considerable research has been conducted on the use of carbon fiber reinforced polymer materials for strengthening and repair of steel beams and flexural members for civil engineering applications [1-4]. This research indicates that conventional modulus CFRP materials can be effectively used to increase the capacity of steel and steel-concrete composite flexural members. However, due to the relatively low modulus of elasticity of conventional CFRP materials, relatively large volumes of CFRP are required to achieve significant stiffness increases. More recently, high modulus CFRP materials have become available with a modulus of elasticity approximately twice that of structural steel. Several researchers [5-8] have indicated that these materials can be effectively used to increase the strength and stiffness of steel-concrete composite beams. Due to the high stiffness of the strengthening materials, plate end debonding is a critical failure mode which should be carefully considered to avoid an undesirable failure of the system. This is particularly important for spliced connections which may be necessary to implement the strengthening system to longer span bridges and structures.

A number of researchers have established analytical models to predict the distribution of shear and peeling stresses near bonded plate ends for both lap shear coupons [9,10] and beams [11-13]. Others have considered a fracture mechanics approach to predict plate end debonding of CFRP plates bonded to steel surfaces [14]. Based on the results of finite element analysis, other researchers have reported that careful detailing of plate ends can significantly reduce bond stress concentrations at these locations, thereby significantly increasing the joint capacity [15,16]. To the authors knowledge, these results have not been verified experimentally, particularly for the case of stiff plates which are commonly used in civil engineering and infrastructure applications.

Research regarding lap spliced connections of plated beams is limited. In one study [17], eight reinforced concrete beams were strengthened with CFRP laminates which incorporated lap-spliced joints at various locations. The research indicates that premature debonding of the splice plates was the primary mode of failure for the tested beams. The

[1]Graduate Research Assistant, mmdawood@ncsu.edu
[2]Distinguished Professor of Civil Engineering and Construction, sami_rizkalla@ncsu.edu

findings of the study indicate that splices should be located such that the maximum longitudinal strain in the CFRP laminate immediately adjacent to the splice should not exceed an experimentally determined limiting value.

This paper presents an extensive experimental program which has been conducted to investigate the bond behavior of CFRP laminates. The paper focuses primarily on plate end debonding of high modulus CFRP plates, particularly as related to spliced connections of strengthening plates installed on steel beams. Several joint configurations are considered in the study and both double-lap shear coupon tests and beam tests are considered and compared.

2 CFRP Strengthening System

The unidirectional CFRP laminates used in the experimental program were manufactured using the high modulus DIALEAD K63712 fibers produced by Mitsubishi Chemical Inc. The material properties of the dry fibers and the pultruded laminates, as reported by their respective manufacturers, are presented in Table 1.

Table 1: Material properties for the dry fibers and the pultruded laminates

Material Property	Dry Fiber [18]	Pultruded Laminate
Elastic Modulus, E	640 GPa	450 GPa
Ultimate Strength, $f_{frp,u}$	2600 MPa	1540 MPa
Ultimate Strain, $\varepsilon_{frp,u}$	0.004	0.0033
Fiber Volume Fraction	N/A	70 %

The CFRP laminates were bonded using Spabond 345, a two part epoxy adhesive, with the fast hardener produced by SP Systems North America. Since the laminates came prefabricated with a roughened surface and a glass fiber peel ply, the surface preparation of the CFRP laminates was minimal. Surface preparation of the steel materials consisted of grit blasting to 'white metal', cleaning by air blowing and solvent wiping. The CFRP strips were installed and clamped for 12 hours until the adhesive had thoroughly set. The adhesive was allowed to cure at room temperature for at least one week prior to testing.

3 Experimental Program

The experimental program was conducted in two phases to investigate the bond and splice behavior of CFRP laminates. In the first phase six double-lap shear coupons with five different joint configurations were tested. The objective of the first phase was to determine the effectiveness of various joint details to help increase the ultimate capacity of bonded splice joints. In the second phase, a total of nine large-scale beam tests were conducted to study the detailed behavior of bonded, spliced connections under flexural loading conditions.

3.1 Double-lap Shear Coupon Tests

A total of six double-lap shear coupons were tested in the first phase of the experimental program. The typical coupons, shown schematically in Fig. 1, consisted of two 8 mm thick x 38 mm wide CFRP main plates which were butted together and connected to each other by two 4 mm thick x 400 mm long CFRP splice plates.

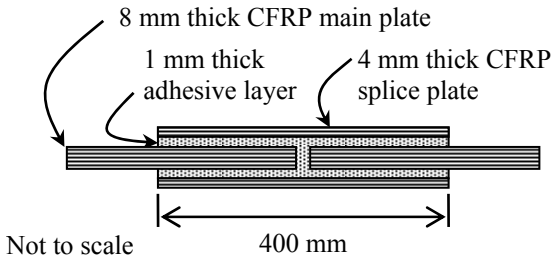

Figure 1: Typical double-lap shear coupon

The test matrix for the double-lap shear coupon tests is presented in Table 2.

Table 2: Double-lap shear coupon test matrix

Specimen ID	Splice Length (mm)	Plate end detail	# of Repetitions
400-S	400	S	1
400-T1	400	T1	1
400-T2	400	T2	2
400-U	400	U	1
400-U-C	400	U	1

Each specimen configuration was assigned a two or three part specimen ID. The first part of the specimen ID indicates the nominal length of the splice plates. The second part of the ID indicates the plate detail at the end of the splice plate and within the center of the joint. A total of four different plate end details were investigated as shown schematically in Table 3. The square end represents the simplest and most commonly used joint detail. To reduce the bond stress concentrations, different combinations of reverse tapered and rounded plate ends were implemented at the end of the splice plate and at the end of the main plate within the center of the joint, as outlined in Table 3. Typical square, tapered and rounded plate ends are shown in Fig. 2 (a), (b) and (c) respectively.

The third part of the ID, denoted by a 'C', indicates the presence of a steel clamp at the ends of the splice plate. The clamp was installed to help resist the peeling stresses which develop near the plate end. The steel clamp is shown in Fig. 2 (d). All of the detailing of the plate ends and of the steel clamps was fabricated using hand tools and simple power tools which are commonly available in most fabrication shops.

Table 3: Plate end details for tested coupons

	End of Splice Plate	Center of Splice Joint
Square (S)	Splice plate Main plate	Splice plate
Tapered 1 (T1)	Adhesive fillet	Splice plate
Tapered 2 (T2)	Adhesive fillet	
Curved & tapered (U)	Adhesive fillet Rounded in plan	Rounded in plan

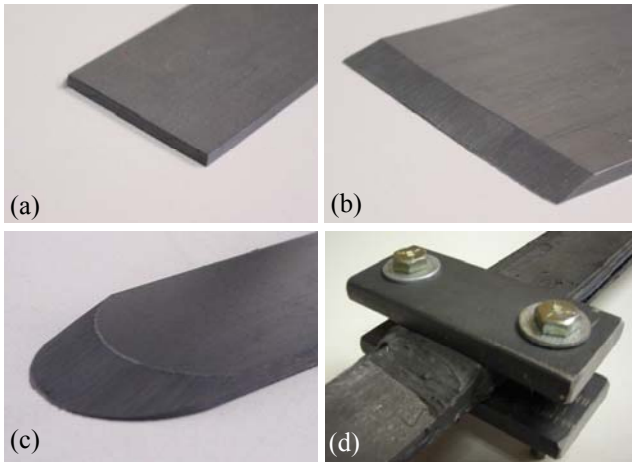

Figure 2: (a) square, (b) tapered, (c) rounded and (d) clamped plate ends

The tension coupons were instrumented with electrical resistance strain gauges, and were loaded monotonically to failure.

3.2 Beam Tests

A total of nine beam tests were conducted in the second phase of the experimental program to investigate the detailed behavior of CFRP splice plates under flexural loading. The typical test beams, shown schematically in Fig. 3, consisted of a W12x30 steel wide flange section. A structural steel channel was welded to the compression flange of the test beam, as shown in Fig. 9, to simulate the presence of a reinforced concrete deck. The beams were strengthened with two CFRP plates which were bonded to the bottom face of the tension flange. The plates were butted at midspan and joined using a bonded CFRP cover plate to simulate a typical field splice. The beams were tested in four-point bending as shown in the figure.

The test matrix for the beam tests is presented in Table 4. The notation used to identify the beam tests is similar to that used in the previous section.

Table 4: Beam test matrix

Specimen ID	Splice Length (mm)	Plate end detail	# of Repetitions
800-S	800	S	2
800-T2		T2	1
800-U		U	1
400-S	400	S	1
400-S-W			1
400-T2		T2	1
400-T2-W			1
200-T2-W	200	T2	1

To help resist peeling stresses near the plate ends, a transverse carbon fiber wrap was installed on three of the tested beams. The presence of the transverse wrap is indicated by a 'W' at the end of the specimen ID. The transverse wrap consisted of dry carbon fiber sheets which extended from the web-to-flange fillet at the top face of the tension flange, around the bottom of the CFRP splice plate, and to the web-to flange fillet on the opposite side of the beam. The fibers were impregnated using the Sika Sikadur 300 impregnating resin. This adhesive was selected on the basis of an extensive adhesive selection study which was conducted in the preliminary stages of this research program [6]. The transverse wrap, shown in Fig. 4, was extended beyond the ends of the splice plate at both ends to ensure adequate anchorage to the tension flange of the beam.

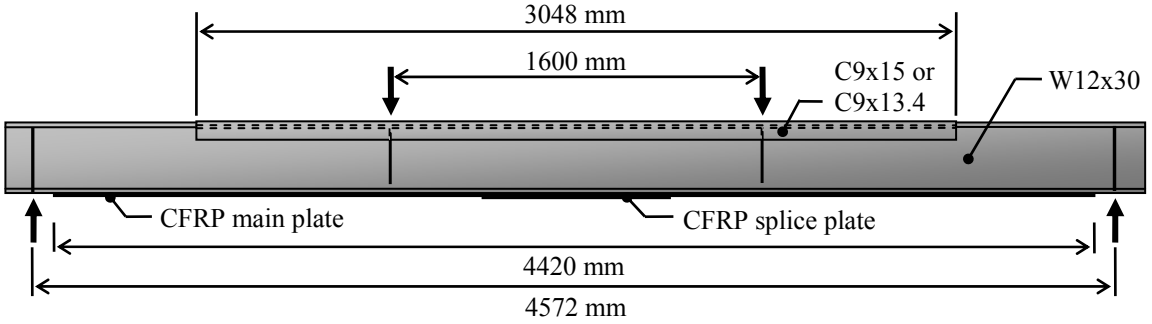

Figure 3: Schematic of test beam and test setup

Figure 4: Transverse fiber wrap

The tested beams were instrumented with linear potentiometers to measure deflections at midspan and at the support locations. Electrical resistance strain gauges were also installed at various locations along the splice plate to evaluate the bond shear stress distribution in the adhesive layer between the CFRP splice plate and the main CFRP plates.

4 Experimental Results

4.1 Double-lap Shear Coupon Test Results

All six of the tested coupons failed by sudden debonding of the CFRP splice plates prior to rupture of the FRP. Typically a mixed mode failure was observed with some adhesive remaining on both the CFRP main plates and on the splice plates as shown in Fig. 5. Inspection of the failure surface suggests that the failure typically occurred within the thin layer of resin left on the surface of the CFRP. The failure surface also exhibited several cracks and diagonal failure planes within the adhesive which suggests a partially cohesive failure. Debonding was accompanied by cracking and splitting of the splice plates due to the sudden nature of the failure.

The maximum load achieved prior to debonding and the maximum measured strain in the CFRP main plate are presented in Table 5 for each of the tested coupons. The numbers in parentheses after the specimen ID indicate multiple repetitions of the same test configuration. The table also presents the ratio of the maximum measured strain in the CFRP main plate, ε_{max}, to the rupture strain of the CFRP, $\varepsilon_{frp,u}$.

Inspection of Table 5 indicates that installation of the reverse taper at the plate ends and within the center of the splice joint, as in configuration 400-T2, approximately doubled the maximum capacity of the bonded joint as compared to the square end configuration, 400-S. Installation of the reverse taper at the end of the splice plate only, configuration 400-T1, increased the ultimate capacity of the joint by 80 percent as compared to the square end configuration. Implementation of the rounded and

Figure 5: Typical failure of splice coupon

Table 5: Double-lap shear coupon test results

Specimen ID	Failure Load (kN)	ε_{max}	ε_{max} / $\varepsilon_{frp,u}$
400-S	89	0.00078	0.23
400-T1	160	0.00129	0.38
400-T2 (1)	191	0.00148	0.44
400-T2 (2)	228	0.00160	0.47
400-U	157	0.00119	0.35
400-U-C	284	0.00200	0.59

tapered plate ends, 400-U, also resulted in an 80 percent increase of capacity. However, it was expected that splice configuration 400-U would exhibit a higher capacity than the configuration with the tapered plate ends, 400-T2. As shown in Table 5, this was not the case. A finite element analysis is currently underway which may provide additional information to help explain the observed behavior. Comparison of the results for configurations 400-U and 400-U-C indicate that installation of the steel clamp near the splice plate ends helped to increase the joint capacity by an additional 80 percent as compared to the unclamped specimen.

Based on the measured strains at various locations along the length of the splice plate, the corresponding longitudinal stress distribution was determined for several of the tested joints. The experimentally obtained stress distribution for coupons 400-S and 400-T2(1), for a load level of 80 kN, are shown in Fig. 6(a) and (b) respectively. The stress distribution was also calculated using an analytical model proposed by Albat and Romily [10] for double-lap shear coupons with square plate ends. The calculated stress distribution is also plotted in the figures for reference purposes.

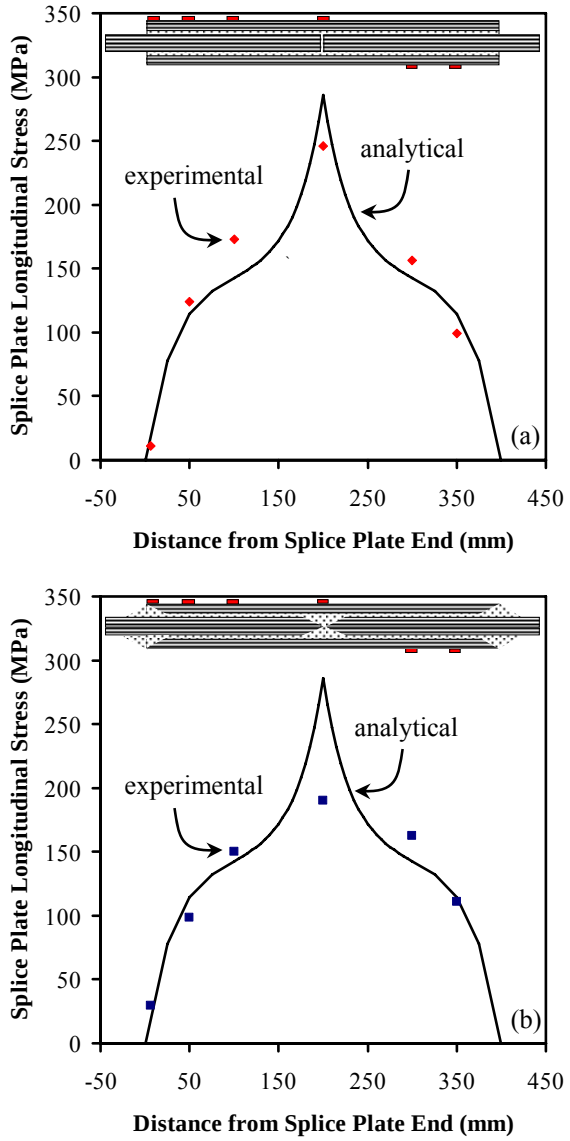

Figure 6: Longitudinal stress distribution in the splice plate for coupon (a) 400-S and (b) 400-T2(1)

Inspection of Fig. 6(a) indicates that the calculated stress distribution closely matches the experimentally obtained stress distribution for joint 400-S. Both the measured and the predicted stress distributions exhibit a sharp peak at the center of the joint, which suggests the presence of a shear stress concentration in the adhesive near this location. Inspection of Fig. 6(b), however, indicates that the measured stress at the center of the splice joint for coupon 400-T2(1), which was fabricated with a reverse taper at this location, was significantly lower than that predicted by the analytical model. This demonstrates that the reverse taper effectively helped to reduce the shear stress concentration which formed near the plate end.

The measured load-strain behavior at the centerline of the splice joint is presented in Fig. 7 for several of the tested specimens. The figure also presents the theoretical load-strain behavior for a continuous 8 mm x 35 mm CFRP plate.

From the figure, it can be seen that the initial response of the joints was linear with a higher stiffness than the theoretical stiffness of the continuous FRP plate. This can be explained by considering the geometry of the spliced joints. Upon fabrication of the splice coupons, a small gap was left between the butted ends of the main CFRP plate, which was subsequently filled with adhesive. This adhesive helped to increase the stiffness at the center of the bonded joint and contributed to the overall splice stiffness.

For the joint configurations 400-S and 400-T1, the high bond stress concentrations near the square plate ends within the center of the joint likely resulted in premature cracking of the adhesive at this location. This can be seen by the sudden increase of the strain at the 40 kN load level in Fig. 7. This increase of strain was accompanied by a corresponding reduction of the stiffness of the joints. Joint 400-T1 exhibited similar increase of strain and further reduction of stiffness at the 150 kN load level. From the figure it can be seen that the final stiffness of joint 400-T1 closely matches the theoretical stiffness of the continuous FRP plate, which indicates that the adhesive at the center of the joint was completely cracked.

Joint configurations 400-T2 and 400-U exhibited slightly different behavior as shown in Fig. 7. The presence of the tapered plate ends within the center of the joint helped to reduce the bond stress concentrations at that location which prevented cracking of the adhesive. Consequently, the joint behavior was linear to failure with a measured stiffness consistently higher than the predicted stiffness.

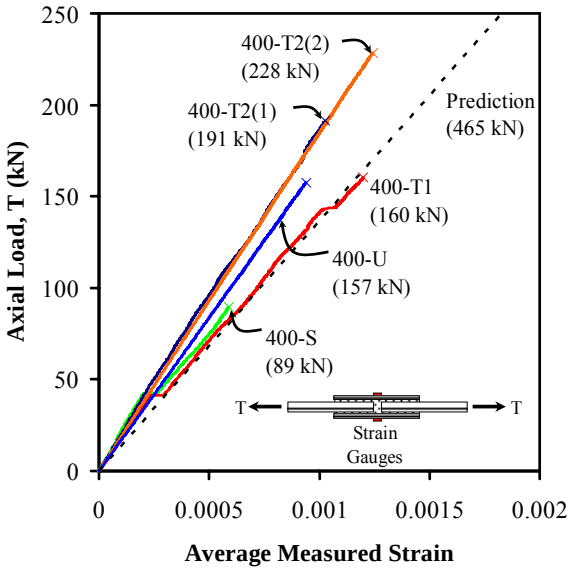

Figure 7: Load-strain behavior at centerline of splice

4.2 Beam Test Results

All of the beams tested in the second phase of the experimental program failed due to sudden debonding of the splice plates as shown in Fig. 8. The failure plane typically extended along the interface between the CFRP splice plate and the CFRP main plate starting

from one end of the splice plate and extending to the center of the splice joint. The debonded region then continued along the interface between the CFRP main plate and the tension flange of the steel beam as shown in Fig. 8. The presence of the transverse wrap on beams 400-S-W, 400-T2-W and 200-T2-W helped to conceal the debonding of the splice plate, however,

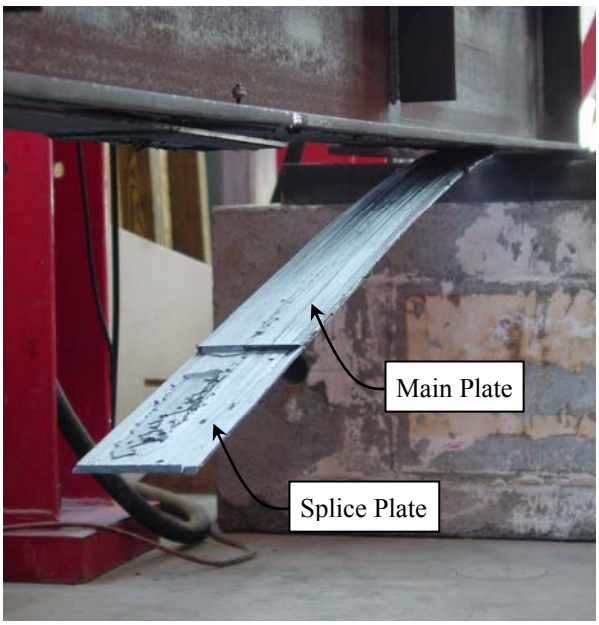

Figure 8: Typical debonding failure of a splice beam

removal of the transverse wrap after failure of the beam revealed a similar failure pattern for these three beams.

The measured load-deflection relationship at midspan is shown in Fig. 9 for each of the tested beams. The dashed line in the figure represents the complete load-deflection relationship calculated using a conventional moment-curvature analysis. From the figure, it can be seen that all of the tested beams failed prior to yielding of the tension flange of the steel beam.

The maximum load achieved prior to debonding and the maximum measured strain in the CFRP main plate are presented in Table 6 for each of the tested beams. The table also presents the ratio of the maximum measured strain in the CFRP main plate, ε_{max}, to the rupture strain of the CFRP, $\varepsilon_{frp,u}$.

A comparison of the maximum load and CFRP strain for beams 400-S, 800-S(1) and 800-S(2) indicates that increasing the splice length from 400 mm to 800 mm did not significantly increase the ultimate capacity of the splice joint for the square ended joints. The longitudinal strains which were measured along the length of the splice plates indicate that these beams exhibited high adhesive shear stress concentrations near the splice plate ends and near the end of the main CFRP plates within the center of the splice joint. The measured stress concentration diminished substantially within the first 100 mm away from the plate ends. These measured localized stress concentrations likely caused the observed debonding failures of the tested

Table 6: Splice beam test results

Specimen ID	Failure Load (kN)	ε_{max}	ε_{max} / $\varepsilon_{frp,u}$
800-S(1)	178	0.00082	0.24
800-S(2)	205	0.00104	0.31
800-T2	408	0.00227	0.67
800-U	343	0.00150	0.44
400-S	180	0.00085	0.25
400-S-W	200	0.00087	0.26
400-T2	340	0.00148	0.44
400-T2-W	218	0.00088	0.26
200-T2-W	236	0.00092	0.27

beams. Consequently, increasing the overall length of the CFRP splice plate beyond 400 mm did not have a significant effect on the joint capacity.

A similar trend was observed for the joints with tapered plate ends, 400-T2 and 800-T2. However, for these beams, decreasing the splice length from 800 mm to 400 mm resulted in a slight decrease of capacity of 17 percent. This indicates that, for the 400 mm splice, there was some interaction between the stress concentration at the end of the splice plate and that at the end of the main CFRP plate. Comparison of the test results further indicates that, for a given splice length, the presence of the reverse tapered plate ends approximately doubled the capacity of the spliced connection which confirms the findings of the double-lap shear coupon tests.

A comparison of the results for beams 800-S(1), 800-S(2), 800-T2 and 800-U indicates that the effect of the plate end details was similar to that observed for the splice coupon tests. This further verifies the trend observed for the splice coupon tests. As previously discussed, the rounded and tapered splice configuration, 800-U, exhibited a lower capacity than the tapered configuration, 800-T2, which was unexpected. The behavior is currently being investigated through a finite element analysis study.

The test results further indicate that installation of the transverse CFRP wrap did not significantly increase the maximum capacity of the spliced joint as can be seen by comparing the results of beams 400-S and 400-S-W. A comparison of the measured failure loads obtained for beams 400-T2 and 400-T2-W indicates a reduction of the measured failure load of 35 percent for the beam which included the transverse fiber wrap. The observed reduction of the ultimate capacity of the splice joint may have been possibly due to a void or a damaged region in the adhesive which may have formed during fabrication of the splice joint. Alternatively, due to the low tensile strength of the transverse fiber wrap in the longitudinal direction of the beam, a crack may have possibly formed in the transverse fiber wrap which could have possibly induced the observed premature debonding failure of the splice joint.

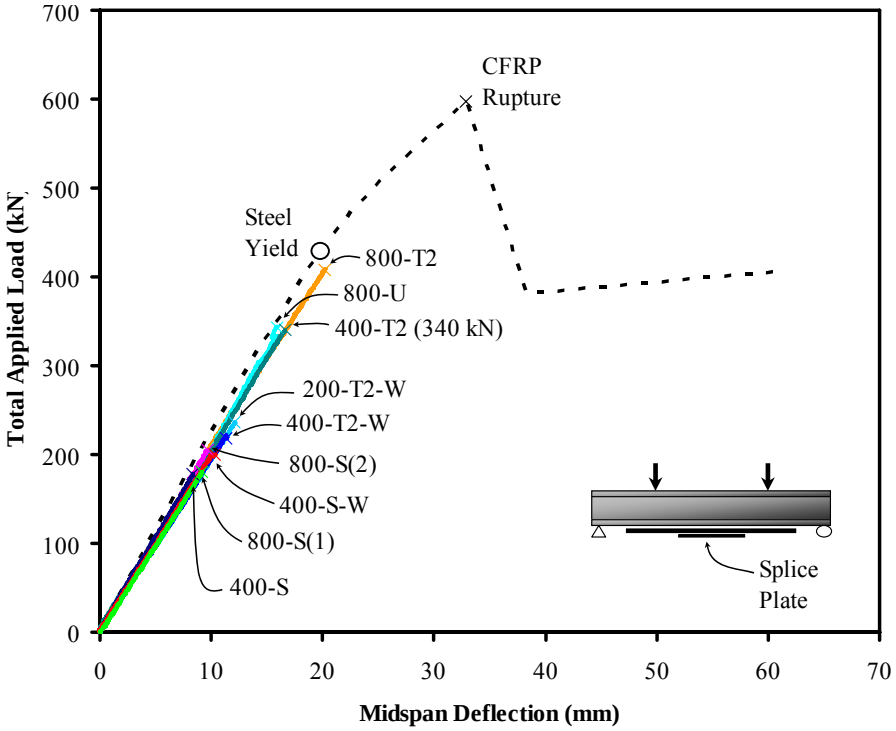

Figure 9: Measured load-deflection relationship for the tested beams

From the longitudinal strain values which were measured along the length of the splice plates, the bond shear stress distribution was determined using Eq. 1,

$$\tau_a = \frac{\varepsilon_2 - \varepsilon_1}{x_2 - x_1} t_{FRP} E_{FRP} \qquad (1)$$

where τ_a is the average adhesive shear stress along a region between adjacent strain gauges, ε_1 and ε_2 are the measured strains at the respective strain gauges, x_1 and x_2 represent the locations of the respective strain gauges and t_{FRP} and E_{FRP} are the thickness and modulus of the CFRP material respectively. The resulting shear stress distributions for beams 400-S and 400-T2 are plotted in Fig. 10(a) for a load level of 120 kN.

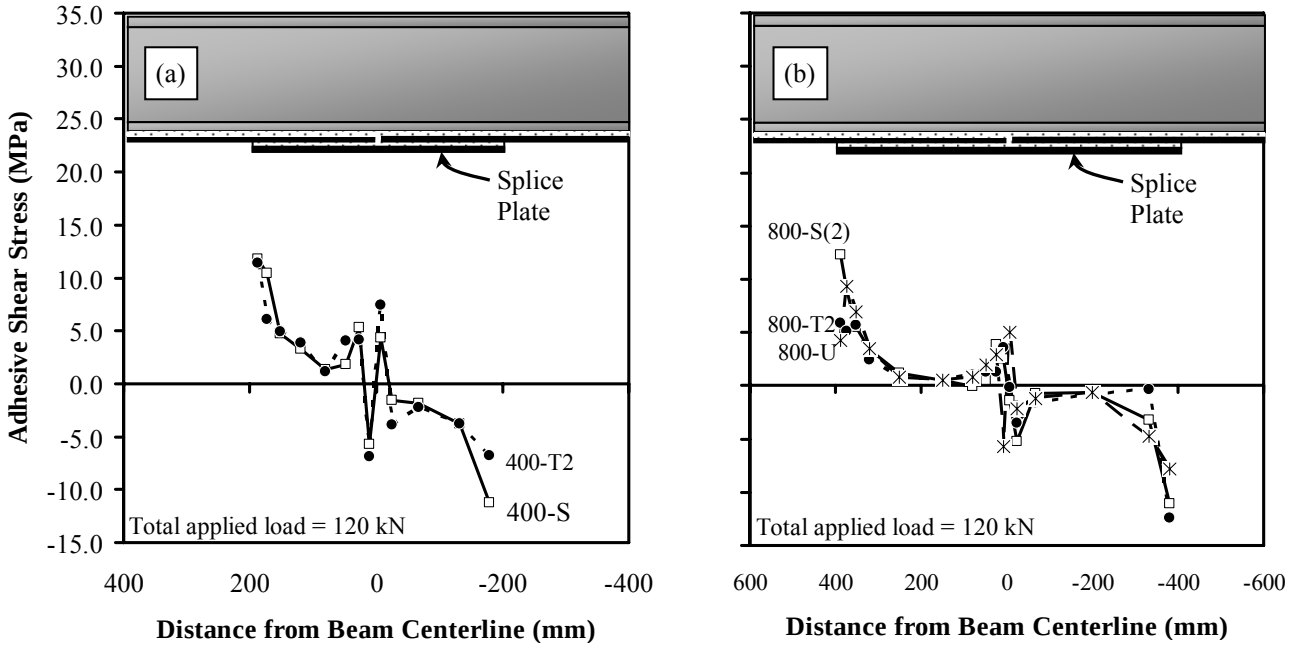

Figure 10: Experimentally obtained adhesive shear stress distributions for the tested beams with (a) 400 mm long splice plate (b) 800 mm long splice plates at a load level of 120 kN

The shear stress distributions for beams 800-S(2), 800-T2 and 800-U are shown in Fig. 10(b). Figure 10 clearly indicates the presence of a bond shear stress concentration near the splice plate ends and near the end of the main CFRP plates. From the figure it is evident that the magnitude of the stress concentration near the splice plate ends was greater than that which occurred near the ends of the main plates. The figure also demonstrates that the presence of the reverse taper near the plate ends typically helped to reduce the magnitude of the observed shear stress concentration for beams 400-T2 and 800-T2. Similarly, the presence of the rounded and tapered plate ends helped to reduce the stress concentrations observed in beam 800-U.

For the beams strengthened with 800 mm long splice plates, the experimentally obtained shear stress decayed to nearly zero at a distance of 200 mm away from the end of the CFRP splice plate, as shown in Fig. 10(b). This indicates that there was no interaction between the shear stress concentrations which formed at the end of the splice plate and at the end of the main CFRP plate. Therefore, the splice length of 800 mm was sufficient to effectively isolate plate ends from each other.

Alternatively, for the beams with 400 mm long splice plates, the bond shear stress did not decay to zero, as seen in Fig. 10(a). This indicates that some interaction between the stress concentrations at either plate end occurred.

The shear stress distributions were also established for the tested beams immediately prior to the observed debonding failure. The stress distributions for the beams strengthened with 400 mm long and 800 mm long splice plates are shown in Fig. 11(a) and (b), respectively. The failure load for each of the beams is noted in parentheses in the figures. For all of the tested beams, failure by debonding typically occurred when the peak shear stress in the adhesive reached a limiting value of approximately 20 MPa, as shown in the figure. Beams 400-T2 and 800-T2, which included reverse tapered plate ends, both achieved peak shear stresses of approximately 35 MPa. It is unlikely that modifying the geometry at the plate end would significantly increase the bond strength of the adhesive. The increase of the observed maximum shear stress for these two beams may have been possibly due to a localized discontinuity in the adhesive which affected the strain locally at the location of the gauges. In any case, the use of a maximum allowable limit for the adhesive shear stress of 20 MPa may be conservative for design purposes based on the observed test results.

5 Conclusions

A total of six double-lap shear coupons and nine steel beams were tested to evaluate the bond and splice behavior of CFRP laminates for strengthening steel beams. The effects of three different parameters were investigated in detail; namely, the length of the CFRP splice plate, the geometric configuration of the plate ends and the presence of additional clamping to resist peeling stresses using steel clamps or transverse fiber wraps. All of the tested specimens failed due to sudden debonding of the splice cover plates.

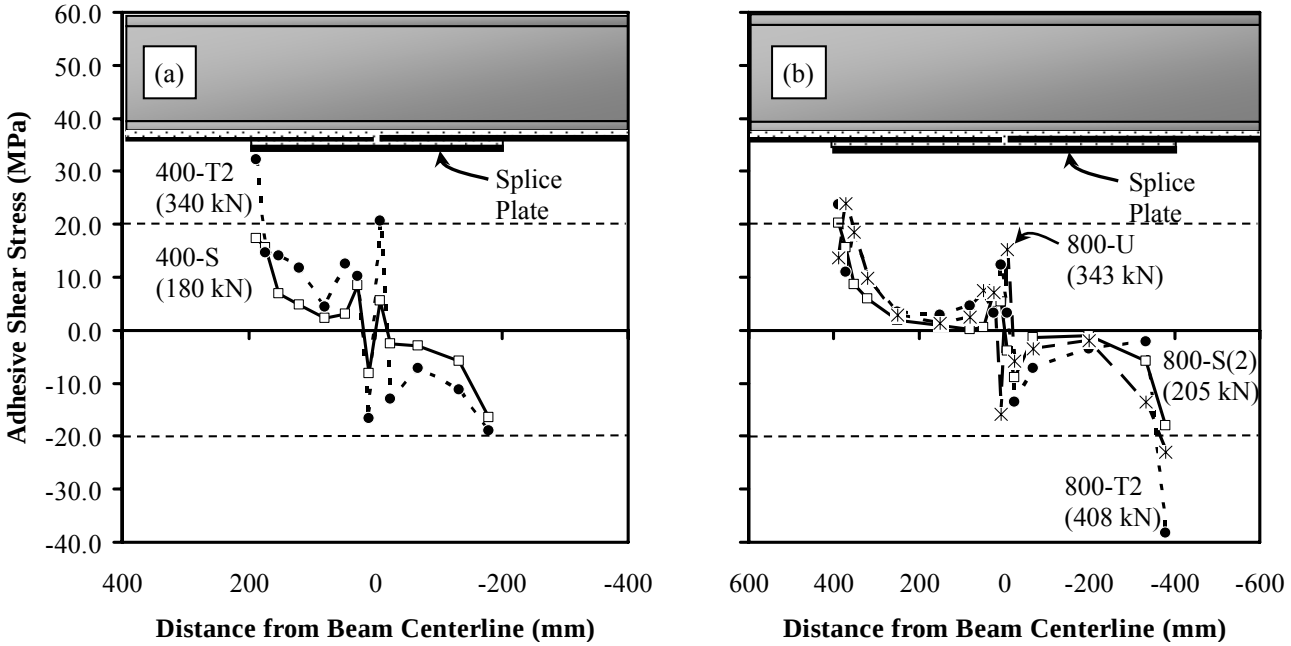

Figure 11: Experimentally obtained adhesive shear stress distributions for the tested beams with (a) 400 mm long splice plate (b) 800 mm long splice plates at failure

Both the double-lap shear coupon tests and the steel beam tests indicated that installation of a reverse tapered plate end can effectively reduce the bond stress-concentrations near the plate end and can help increase the debonding strength of a typical spliced connection. For the tested strengthening system, the specimens that implemented the reversed tapered joint configuration exhibited a maximum capacity at debonding approximately twice that of similar specimens with square plate ends. Similar results were obtained for specimens using rounded and tapered plate ends, however, the observed strength increase was only about 80 percent as compared to specimens with square plate ends.

The research further indicates that providing a steel mechanical clamp near the plate ends can help to resist the peeling stresses which form near the plate end. The use of a steel clamping system helped to increase the maximum capacity of one of the tested double-lap shear coupons by 80 percent as compared to a similar coupon tested without the steel clamp. The beam test results indicate that installation of a transverse CFRP wrap did not significantly increase the joint capacity.

The experimental results also demonstrate that, for the specific strengthening system tested, increasing the splice length beyond 400 mm does not significantly increase the ultimate strength of bonded splice joints with square plate ends and only has a relatively small effect for splices with reverse tapered plate ends.

Typically for the tested beams, a maximum shear stress of 20 MPa was observed immediately prior to debonding. This may represent a reasonable upper limit for the allowable adhesive shear stress for the strengthening system tested.

Based on the findings of the current study, it is evident that careful design and detailing of bond splice joints is essential to ensure satisfactory performance of the joint. To help maximize the capacity of bonded joints, all plate ends should implement a reverse tapered detail. Additional use of a mechanical clamping system can also help to increase the joint capacity. The findings of this paper demonstrate that using simple detailing, the capacity of a bonded splice joint can be increased dramatically as compared to the typical square end configuration which is currently in common use.

Acknowledgements

The authors would like to acknowledge the generous support of Mitsubishi Chemical FP America Inc. and the National Science Foundation (NSF) Industry/University Cooperative Research Center (I/UCRC) on Repair of Buildings and Bridges with Composites (RB^2C).

References

[1] Sen, R. & Libby, L. (1994). *Repair of steel composite bridge sections using CFRP laminates.* Final report submitted to Florida and US Department of Transportation. Virginia: NTIS.

[2] Mertz, D.R. & Gillespie Jr., J. W. (1996). *Rehabilitation of steel bridge girders through the application of advanced composite materials* (Contract NCHRP-93-ID011). Washington, D.C.: Transportation Research Board.

[3] Tavakkolizadeh, M. & Saadatmanesh, H. (2003c). Strengthening of steel-concrete composite girders using carbon fiber reinforced polymer sheets. *Journal of Structural Engineering*, 129 (1), 30-40.

[4] Al-Saidy, A.H., Klaiber, F.W. & Wipf, T.J. (2004). Repair of steel composite beams with carbon fiber-reinforced polymer plates. *Journal of Composites for Construction*, 8 (2), 163-172.

[5] Dawood, M. (2005). *Fundamental Behavior of Steel-Concrete Composite Beams Strengthened with High Modulus Carbon Fiber Reinforced Polymer Materials.* Master's Thesis, North Carolina State University.

[6] Schnerch, D. (2005). *Strengthening of steel structures with high modulus carbon fiber reinforced polymer (CFRP) Materials.* Ph.D. dissertation, North Carolina State University, Raleigh, North Carolina.

[7] Schnerch, D., Dawood, M., Rizkalla, S. and Sumner, E. (2006). Proposed design guidelines for strengthening of steel bridges with FRP materials. *Construction and Building Materials*, accepted for publication

[8] Shaat, A. and Fam, A. (2006). Rehabilitation of damaged steel-concrete composite beams using high modulus CFRP sheets. In the *Proceedings of the 7th international conference on short and medium span bridges, Montréal, Canada, August 23-26, 2006* [CD-ROM]. Montréal, Canada: CSCE.

[9] Cadei, J.M.C., Stratford, T.J., Hollaway, L.C. & Duckett, W.G. (2004). *Strengthening metallic structures using externally bonded fibre-reinforced polymers.* London, England: CIRIA.

[10] Albat, A.M. & Romily, D.P. (1999). A direct linear-elastic analysis of double symmetric bonded joints and reinforcements. *Composites Science and Technology*, 59, 1127-1137.

[11] Täljsten, B. (1997). Strengthening of beams by plate bonding. *Journal of Materials in Civil Engineering*, 9 (4), 206-212.

[12] Smith, S.T. & Teng, J.G. (2001). Interfacial stresses in plated beams. *Engineering Structures*, 23, 857-871.

[13] Stratford, T & Cadei, J. "Elastic analysis of adhesion stresses for the design of a strengthening plate bonded to a beam," *Construction and Building Materials*, v. 20, 2006, pp. 34-45.

[14] Lenwari, A., Thepchatri, T and Albrecht, P. (2006). "Debonding Strength of Steel Beams

Strengthened with CFRP Plates," ASCE Journal of Composites for Construction, v. 10, no. 1, January/February, pp. 69-78.

[15] Hildebrand, M (1994). Non-linear analysis and optimization of adhesively bonded single lap joints between fibre-reinforced plastics and metals. *International Journal of Adhesion and Adhesives,* 14, 4,, 261-267.

[16] Belingardi, G., Goglio, L. and Tarditi, A. (2002). Investigating the effect of spew and chamfer size on the stresses in metal/plastics adhesive joints. *International Journal of Adhesion and Adhesives,* 22, 273-282.

[17] Stallings, M. and N. M. Porter (2003). Experimental investigation of lap splices in externally bonded carbon fiber-reinforced plastic plates. *ACI Structural Journal,* 100, 1, 3-10.

[18] Mitsubishi Chemical FP America Inc. (2004). *Dialead: High performance coal tar pitch based carbon fiber.*